

# Piezoelectric Energy Harvesting Technology: From Materials, Structures, to Applications

Tao Li and Pooi See Lee\*

The piezoelectric energy harvesting is a promising, interesting and complex technology. Herein, the aim is to review the key groups of parameters that contribute to the performance of energy harvesting and to offer a guideline for the future development. For this purpose, a universal theoretical model is developed. According to the model, the parameters are divided into six groups. Each group is then discussed. First, a discussion on the piezoelectric materials status, advantages and disadvantages of ceramics, polymers, single crystals, composites, nanomaterials, and lead-free materials are summarized. The orientation of materials is also discussed. Second, the structure designs, including off-resonance, on-resonance, and impact design were introduced. Third, typical sources of excitations and vibrations are given, including direct contact force, low vibration force, hydraulic, pneumatic power, and acoustic power. The fourth consideration is on the effect of frequency and speed is discussed, focusing on the high-frequency and high-speed conditions. This is followed by the effect of electrical load on the output power of an energy harvester was discussed. Last, the parameters of energy accumulation effect and methods are also introduced. Following the above discussion, some examples are provided to show the potential applications, including the areas of structural health monitoring, vibration engines, pavement road energy harvesting, wireless sensor nodes, and human gait power. Finally, at the end of the review, the future challenges are addressed.

## 1. Introduction

Piezoelectric energy harvester is the device which uses the external force acting on the piezoelectric elements to generate energy. Usually, this technology is used to convert the ambient waste energy into the usable electrical energy. The mechanism of piezoelectric energy harvester is based on the direct piezoelectric effect. When the harvester is subjected to the stresses, charges will be generated on the materials surface proportionally. When connected to external circuit, the charges will lead to current flow through the load. Therefore, the piezoelectric material in this operation is essentially a voltage, current, charge, or power source. Sometimes, the piezoelectric energy harvester is also called energy scavenger or power generator. Conventionally, the direct piezoelectric effect is applied in piezoelectric sensors, for example, force, pressure and acceleration sensors. In recent decades, the application of direct piezoelectric effect on energy harvester has drawn increasing attention due to a few reasons: first, this is the response of energy crisis.

There are increasing concerns on the energy depletion and the need for carbon emission reduction. Therefore, interests on replacement energy over the existing fossil fuel energies arise. Second, environment issue calls for clean, green, sustainable and reusable energy. The present era of industrialization is most advanced than ever in the history, however, the release of waste also brings significant environmental problems. Last but not least, in recent decades, the development of smart devices is rapid and adoption is widespread. Many of them requires low power or powerless for applications such as medical, mobile, or remote devices, where the change of battery is not convenient, high labor cost, inaccessible, or with great hassles.

So far there are different kinds of ways for energy harvesting, for example, wind power, hydraulic power, solar power and thermal power etc. Piezoelectric energy harvester is materials based power generator. It features low profiles, micro to meso scale, flexible in structures designs, long life span, and thus is a good candidate for small devices applications. The power level of an energy harvester usually falls in the order of nW,  $\mu$ W, mW, or W.<sup>[1]</sup> In the process of energy harvesting, the mechanical energy is converted into the electric energy. The energy output of the device is related to a number of parameters. Figure 1a is the equivalent circuit model of the piezoelectric energy harvester,

---

T. Li, P. S. Lee  
School of Materials Science and Engineering  
Nanyang Technological University  
Singapore 639798, Singapore  
E-mail: PSLee@ntu.edu.sg

T. Li, P. S. Lee  
Singapore-HUJ Alliance for Research and Enterprise (SHARE)  
Nanomaterials for Energy and Energy Water Nexus (NEW)  
Campus for Research Excellence and Technological Enterprise  
Singapore 138602, Singapore

 The ORCID identification number(s) for the author(s) of this article can be found under <https://doi.org/10.1002/sstr.202100128>.

© 2022 The Authors. Small Structures published by Wiley-VCH GmbH. This is an open access article under the terms of the Creative Commons Attribution-NonCommercial-NoDerivs License, which permits use and distribution in any medium, provided the original work is properly cited, the use is non-commercial and no modifications or adaptations are made.

DOI: [10.1002/sstr.202100128](https://doi.org/10.1002/sstr.202100128)

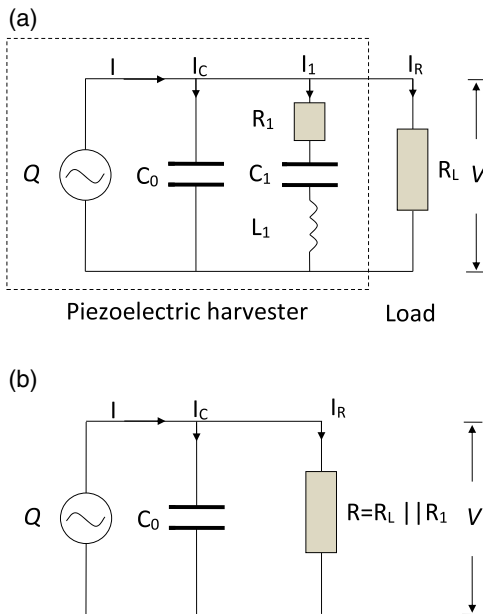


**Figure 1.** a) Equivalent circuit b) and simplified model of the energy harvester.

in which,  $Q$  is the charge generated due to the force  $F$  acting on the piezoelectric element,  $C_0$  is the static capacitance,  $R_1$ ,  $C_1$ , and  $L_1$  is equivalent resistance, capacitance and inductance at the mechanical series resonance, and  $R_L$  is the external load resistance. In the mechanical branch  $I_1$  of the harvester, the impedance can be expressed as

$$Z = R_1 + j \left( \omega L_1 - \frac{1}{\omega C_1} \right) \quad (1)$$

It is well known that during resonance, there is

$$\omega L_1 = \frac{1}{\omega C_1} \quad (2)$$

So the impedance  $Z$  reduces to  $R_1$  only. As a result, Figure 1a can be simplified to Figure 1b. This model is essentially similar as the one in ref. [2] for the off-resonance conditions. Therefore, both the on-resonance and off-resonance piezoelectric harvester can be represented using the same model, especially for qualitative analysis. In the following part, Figure 1b is just applied to reveal the key parameters of the piezoelectric energy harvester.

According to Figure 1b,  $I_c$  and  $I_R$  in parallel, so

$$Z_{C||R} = \frac{Z_{C0} \times R}{Z_{C0} + R} \quad (3)$$

The voltage across  $R$  is then

$$V = I \times Z_{C||R} = \frac{j\omega QR}{1 + j\omega C_0 R} \quad (4)$$

$C_0 R$  is the so-called time constant  $\tau$ , therefore

$$|V| = \frac{Q}{C_0} \frac{\omega \tau}{\sqrt{1 + (\omega \tau)^2}} \quad (5)$$

The corresponding current flowing through  $R$ , then becomes

$$|I| = \frac{|V|}{R} = \frac{Q}{C_0} \frac{\omega \tau}{\sqrt{1 + (\omega \tau)^2}} \times \frac{1}{R} \quad (6)$$

The power can be calculated to be

$$P = \frac{|V|^2}{R} = \left( \frac{Q}{C_0} \frac{\omega \tau}{\sqrt{1 + (\omega \tau)^2}} \right)^2 \times \frac{1}{R} \quad (7)$$

The energy is then

$$E = P \times T = \left( \frac{Q}{C_0} \frac{\omega \tau}{\sqrt{1 + (\omega \tau)^2}} \right)^2 \times \frac{1}{R} \times T \quad (8)$$

$T$  is the time. Taking in the following expression

$$Q = dF \quad (9)$$

$$C_0 = \epsilon \frac{A}{t} \quad (10)$$

The energy finally becomes

$$E = \left( \left( \frac{d}{\epsilon} \right)^2 \right)_1 \times \left( \left( \frac{t}{A} \right)^2 \right)_2 \times (F^2)_3 \times \left( \left( \frac{\omega \tau}{\sqrt{1 + (\omega \tau)^2}} \right)^2 \right)_4 \times \left( \frac{1}{R} \right)_5 \times (T)_6 \quad (11)$$

In the above expression,  $d$  is piezoelectric charge coefficient  $\epsilon$  is dielectric constant,  $t$  is the thickness and  $A$  is the area of the sample. This equation reveals that the output of an energy harvester is essentially determined by a few groups of parameters. They are the materials properties as indicated in (1), structure design properties as indicated in (2), external force and excitations as indicated in (3), working frequency or speed as indicated in (4), electrical load as indicated in (5), and time as indicated in (6).

This equation is the general expression of output of an energy harvester. It does not cover the details of a specific design. It reveals the key parameters that the output of a harvester is related with. To note that those parameters may link together, for example, the structural design affects not only the mechanical resonance, but also the electrical optimal electrical load. As the consequence, in the practical design, they shall all be included in the design scheme. In practice, many authors also apply the concept of normalized energy density, for example, power density per unit area or volume, for comparison purpose.<sup>[3]</sup> Previously, there have been some authors who reviewed the development and recent progress of piezoelectric energy harvesters with different focusing aspects.<sup>[4]</sup> For example, Liu et al.

reviewed a few performance enhancement technologies on energy harvesters.<sup>[4a]</sup> Banerjee et al. reviewed the lead-free materials.<sup>[4b]</sup> And Tian reviewed the MEMS scale piezoelectric energy harvester.<sup>[4c]</sup> Different from those revisions, in this article, we first derive the universal modeling of the piezoelectric energy harvesters as indicated above. From there, we group and explicitly express the key parameters. From this expression, the contribution of each group's parameters on the performance of energy harvesting can be clearly seen. Thereafter, we made detailed discussions on each group of parameters, i.e., materials, structural design, external force, frequencies, load and time. Examples of potential applications were also provided.

## 2. Materials

The first factor in the previous Equation (11) is the group of material properties. Regarding this, two aspects shall be considered. The first one is the types of materials. The second one is the orientation of the materials. For the former, many categories of materials have been explored for the application of energy harvesters. They might be classified generally as ceramics, polymers, composites, single crystals, nano-materials, and lead-free materials etc. In the previous part, we have given an illustrative modeling. In ref. [5], some modeling and predictions were also provided. They proposed the parameter called dimensionless figure of merit (DFOM) as a criterion for energy harvester material selection. A 31-mode piezoelectric harvester can be expressed as

$$\text{DFOM} = \left( \frac{k_{31}^2 \cdot Q_m}{s_{11}^E} \right)_{\text{on-resonance}} \left( \frac{d_{31} \cdot g_{31}}{\tan\delta} \right)_{\text{off-resonance}} \quad (12)$$

This expression is more complete and explicit. And it can be a good guide for estimate and analyze different materials.

Regarding the orientation of the materials, the piezoelectric material is in nature anisotropic. Different alignment of the direction in the device, the obtained properties will be different. For example, taking the well-accepted PZT materials, after poling, the symmetry is axisymmetric. Therefore, accordingly there exists 31-mode, 33-mode, and 15-mode designs of the devices.

**Table 1.** Performance parameters of commonly used piezoelectric materials.<sup>[7]</sup>

Parameter	Inorganic							
	Single crystal				Bi crystal		Organic PVDF	Composite P(VDF-TrFE)
	Quartz crystal	PZT-4	PZT-5 A	PZT-5 H	PZT-8	ZnO		
K	0.06	0.89	0.95	0.1	0.8	–	–	14
$d_{31}$	–0.67	–123	–171	–274	–97	–5	–5.43	–20
$d_{33}$	2.3	289	374	593	225	12.4	5	30
$E_r$	4.6	38	50	100	29	–	8.5	12.15
$\tan\delta$	–	0.004	0.02	0.02	0.004	–	–	0.018
$Q_m$	100	500	75	600	1000	1770	2490	3500
E [GPa]	77.8	76.5	61	49		210	310	2.8
$\nu$	0.17	0.32	0.31	0.36	0.3	0.33	0.25	0.33
$P$ [Kg m <sup>–3</sup> ]	2650	7500	7750	7500	7600	5660	3260	1750
								1890

the parameter of FOM as  $k_{31}^2 \times d_{31} \times g_{31}$  for off-resonance condition,  $k_{31}^2$  for type-1 harvester, and  $(k_{31}^2 \times Q_m)/s_{11}^E$  for type-2 harvester. The work infers that if the mechanical and electrical loss is low, soft materials provide higher performance for the on- or off-resonance conditions. On contrary, if the loss is high, hard material gives higher performance. Neiss et al. supports similar proposition that hard material is better for large amplitude resonance applications.<sup>[9]</sup> The parameters  $d_{33}$  and  $\epsilon$  are the important parameters for the materials selection.<sup>[10]</sup> PZT-51 has been shown to be is a good soft material for energy harvester applications.<sup>[10]</sup>

The output capability of PZT materials is diverse depending on the testing conditions. An example is provided in ref. [11], in which the output performance is reliant more on the materials and less on the structures. In the article, the piezoelectric disk samples with thickness 1.5 mm and diameter 8, 13, and 29 mm were applied with force 100–500 N at 0.5–0.8 Hz and 33 direction. Maximum 2.5  $\mu$ W power output, and nearly 8 V voltage was obtained. A higher  $d_{33}g_{33}$  results in higher output. From the testing of a 31-mode PZT plate with dimensions  $18 \times 5 \times 5$  mm<sup>3</sup>, about 1.2 mW power was obtained with four parallel PZT and 1 Hz.<sup>[12]</sup> The PZT multilayer stack (32.4  $\times$  7.1  $\times$  7.6 mm<sup>3</sup>) tested in a wideband frequency from 1 to 20 000 Hz.<sup>[13]</sup> Compared with the previous examples, 30.7 mW in off-resonance and 347 mW in on-resonance condition was achieved.<sup>[13]</sup> Notably, 35% efficiency was obtained, and 6600  $\mu$ F capacitor was quickly charged within order of seconds. As we have mentioned earlier, the output of harvester is related to many parameters. These examples show that the PZT material is versatile and suits different level of power generators.

### 2.1.2. Polymers

Poly(vinylidene fluoride) (PVDF), and copolymers poly(vinylidene fluoride-trifluoroethylene) (P(VDF-TrFE)) are the most popular piezoelectric polymer materials. Different from ceramics, they provide lower piezoelectric coefficients, yet the polymer endow larger mechanical flexibilities, lower stiffness and higher chemical resistance, which prevent fatigue and increase the lifetime of the device.<sup>[10,14]</sup> Typical materials properties can be found in Table 1. PVDF and copolymers can be used for sensors, actuators, and also the energy harvesters. Some of the relevant advantages of the PVDF materials will be shown in the following examples.

A MEMS scale energy harvester using the PVDF-TrFE materials was fabricated.<sup>[15]</sup> Standard MEMS technique was applied for fabrication on Si substrate. The harvester has a cantilever and proof mass structures. The piezoelectric layer is spin coated with thickness of 1.3  $\mu$ m. The electrode is based on sputtered Al and Ti/Al thin film, and the performance was measured using the press and release method. The maximum power output was found to be 35.1 pW for a tip displacement of 500  $\mu$ m from a 1200  $\times$  300  $\mu$ m<sup>2</sup> cantilever, corresponding to a power density 97.5 pW mm<sup>-2</sup>. One of the important advantages of the harvester is that, the PVDF-TrFE materials have low crystallization temperature (160 °C), which makes it much more compatible with CMOS technology or flexible electronics than the ceramics materials. So the PVDF-TrFE based piezoelectric energy harvesters are suitable candidates to create self-sustained lower power electronics.

A backpack energy harvester using the piezoelectric PVDF strap was created.<sup>[16]</sup> The normally used fabric straps are replaced with the PVDF polymer strap, exploiting the advantages of flexibility and durability of PVDF material. The PVDF strap generates energy when strained during walking. The strap can be arranged parallel or series for maximum energy output. The maximum instantaneous power 0.345 W and average power 45.6 mW were predicted by the authors.

### 2.1.3. Lead-Free Materials

Lead-free materials draw attention due to the environmental issues in the recent decades. The normally used PZT ceramics contains toxic lead. Many researchers hence devote efforts to explore the replacement materials to meet the environmental regulations for new applications. The lead-free materials can be classified into organic and inorganic materials.<sup>[3b,17]</sup> The PVDF and copolymers are the organic materials. The inorganic lead-free materials can be categorized as tungsten bronze, aurivillius (bismuth layer structured ferroelectrics), and perovskite families.<sup>[17b]</sup> BT (Barium titanate), BNT (Bismuth sodium titanate), KNN (sodium potassium niobate), and their derivatives are the actively studied lead-free compositions with perovskite structures.<sup>[17]</sup> The BT-based ceramics was the first reported lead-free piezoelectric ceramics and KNN is considered as one of the most promising lead-free materials.<sup>[17]</sup>

BaTiO<sub>3</sub>-based ceramics with doping have been studied and compared with PZT.<sup>[18]</sup> The composition of the studied materials is BaTiO<sub>3</sub>, Mn-doped BaTiO<sub>3</sub>, and Mn-doped (Ba<sub>0.85</sub>Ca<sub>0.15</sub>)(Ti<sub>0.95</sub>Zr<sub>0.05</sub>)O<sub>3</sub>. The unimorph sample attached with the self-fabricated and commercial PZT were tested at off-resonance frequency of 80 Hz. The results indicate that hard materials which has a higher coercive field exhibit larger voltage and energy. The Mn-0.2 mol% doped BaTiO<sub>3</sub> ceramics unimorphs with the size  $18 \times 10 \times 0.5$  mm and  $Q_m$  of 95.3 generated 432  $\mu$ J energy under experimental conditions of 45 s oscillation, 0.8 mm displacement, and 80 Hz frequency. This result is approximately one-fourth of the PZT materials. The performance is relatively modest, however, it is lead free and thus considered to be valuable.

A series of  $(1-x)$ Bi<sub>0.5</sub>Na<sub>0.5</sub>TiO<sub>3</sub>-xBaTiO<sub>3</sub> ( $0 \leq x \leq 0.1$ ) piezoelectric ceramics for energy harvesting applications has been investigated.<sup>[19]</sup> The materials were prepared with the conventional mixed oxide method and sintered in the range from 1100 to 1200 °C. It was found that the BT content affects the performance of the materials. When the content is  $x = 0.04$ , a piezoelectric voltage coefficient of  $47.03 \times 10^{-3}$  Vm N<sup>-1</sup> can be obtained, which is slightly higher than the PZT-based ceramics. When the content is  $x = 0.06$ , the maximum charge coefficient and output voltage of 164 pC N<sup>-1</sup> and 8.95 V can be obtained. And when  $x = 0.08$ , highest output power of 18 nW was achieved. The author claims lead-free  $(1-x)$ Bi<sub>0.5</sub>Na<sub>0.5</sub>TiO<sub>3</sub>-xBaTiO<sub>3</sub> piezoelectric ceramics are good candidates for energy-harvesting applications.

The CuO-added (Na<sub>0.5</sub>K<sub>0.5</sub>)NbO<sub>3</sub> (CNKN) materials are reported in ref. [20] as promising candidate for piezoelectric energy harvesting and were compared with PZT and NKN (or KNN). The materials were prepared using the mix oxide method. The cantilever harvester was applied for the performance testing.

**Table 2.** Comparison of NKN and CNKN.<sup>[7]</sup>

	NKN	CNKN
$k_p$	0.37	0.38
$Q_m$	65	803
Dielectric loss [%]	3.1	0.9
$d_{33}$ [pC/N]	123	100
3/0	340	230
$d_{33} \times g_{33}$ [ $10^{-15} \text{ m}^2 \text{ N}^{-1}$ ]	5026	4911
$\eta$	0.84	0.99
D OM	139	6083 <sup>a)</sup>
-	-	7356 <sup>b)</sup>

<sup>a)</sup>Calculated using  $s_{11}^E$  value of NKN ceramics; <sup>b)</sup>Calculated using  $s_{11}^E$  value of KCN-doped NKN ceramics.

The materials properties obtained are shown in Table 2. CNKN has similar  $d_{33} \times g_{33}$ , however larger DFOM (dimensionless figure of merit) and  $\eta$  (energy convergence efficiency) due to larger  $Q_m$  and smaller dielectric loss. Compared with most of PZT-based ceramics, CNKN exhibits smaller  $d_{33} \times g_{33}$ , however much larger DFOM and  $\eta$ . The CNKN exhibited a high output power density of  $12 \text{ mW cm}^{-3}$  at 93 Hz and 250 kΩ resistance. The authors claim that the performance is similar to PZT-based energy harvester and CNKN is good candidate for energy harvesters.

The perovskite lead-free piezoelectric materials have been studied over years. Many improvements or advantages have been shown or explored. For example, the system  $(1-x)\text{Ba}(\text{Zr}_{0.2}\text{Ti}_{0.8})\text{O}_3\text{-}x(\text{Ba}_{0.7}\text{Ca}_{0.3})\text{TiO}_3$  shows both high dielectric constant ( $\epsilon_r = 3060$ ) and piezoelectric coefficient ( $d_{33} = 620 \text{ pC N}^{-1}$ ) at  $x = 0.5$ . This is comparable to those of soft PZT materials.<sup>[17b]</sup> Another example, the Mn-modified BNT-based system exhibited relatively small decrease in  $Q_m$  with vibration velocity, resulting in higher maximum vibration velocity than hard PZT ceramics. This property will be an advantage for higher frequency and higher amplitude energy harvester applications. The density of KNN (hot press) is about  $4.46 \text{ g cm}^{-3}$ , which is also lower than PZT ( $7.8 \text{ g cm}^{-3}$ ).<sup>[17b]</sup> So this is naturally advantageous for portable or wearable energy harvester applications. However, even though the lead-free materials has begun to show some superior aspects, the overall properties of the present lead-free materials are still inferior to those of the PZT ceramics,<sup>[17b]</sup> such as lower piezoelectric properties (Table 1 and 2), lower thermal stability, difficulty in processing and so on. Some methods of improvement have been proposed in ref. [17b], for example, composition modification by doping, composition modification by solid solutions, microstructure modification, and MPB modification. To completely replace the PZT ceramics, there is still a long way to go currently. However, it may start from some specific scenarios, for example, when the environmental compatibility is the major concern.

#### 2.1.4. Piezoelectric Nanomaterials

Piezoelectric nanomaterials and structures have attracted increasing interests in the recent years.<sup>[21]</sup> Zinc oxide is a typical

representative of the nano-materials. It is an abundant natural metal oxide, low cost, chemically stable in air and biologically safe.<sup>[21a]</sup> The most common phase is hexagonal wurtzite structure.<sup>[21a]</sup> Zinc oxide is not ferroelectric. The nanostructure can be formed relatively easily using the low temperature method in various flexible and rigid substrate, and no poling process is required.<sup>[22]</sup> Some of the piezoelectric properties of the ZnO have been shown in the previous Table 1. It is not comparable with PZT. However, various nanostructures can be easily formed, for example, lateral nanorods, tilted nanorods, vertical nanorods, nanotubes, and nanowires.<sup>[21–23]</sup> Those structures may generate DC or AC voltage upon the external stresses.<sup>[23a]</sup> The energy-harvesting capability has been examined extensively. Some examples are discussed in the following.

A tuning fork type ZnO nanogenerator was developed.<sup>[24]</sup> The vertical nanorods functional microstructures were grown on a flexible Kapton substrate through a low temperature hydrothermal method. The tuning shape was designed to reduce the vibration frequencies. The generator shows a few advantages, for example, flexible, low resonant frequency, easy manufacturing process, and higher robustness. The generator was tested in a vibrator. It was found that the resonant frequency is 13 Hz, the peak output voltage and current could respectively reach about 160 mV and 11 nA and a maximum instantaneous peak power of  $0.92 \mu\text{W cm}^{-3}$  across a matched load of  $9 \text{ M}\Omega$ .

Laterally aligned nanowires in a PI-NF-PI sandwich structure can be found in ref. [25]. The solvothermally grown nanowires have small diameters 10–50 nm and high aspect ratio  $>20$ . The entire device is flexible and can be bent freely. The generator is delivers positive output voltage 0.127 V upon upward bending, and  $-0.166 \text{ V}$  upon downward bending. The circuit output current is 10 nA. The power density is about  $10 \mu\text{W cm}^{-3}$ .

A ZnO wearable energy harvester was developed using nylon fabric as the substrate, which was fabricated with vertical nanorods structures through the hydrothermal methods.<sup>[26]</sup> The nanorods are 4 μm in length and 100 nm in diameters. The generator is able to generator voltage 4, 0.8 V, current 10 nA, 5 nA under palm clapping and finger bending test, respectively. The life time test shows over 1000 cycles, the degradation is acceptable.

**Table 3.** Properties of piezoelectric samples.<sup>[28]</sup>

Material	PZT-5 H	PMN-33% PT[001]	PZN-6% PT[011]
Dielectric constant $\epsilon_{33}^T/\epsilon_0$ [1 kHz]	3270	6080	6099
Dielectric loss $\tan\delta$	0.016	0.0042	0.0047
Electromechanical coupling factor	$K_{31}$ 0.52	$K_{31}$ 0.62	$K_{32}$ 0.877
Piezoelectric charge constant [pC N <sup>-1</sup> ]	$d_{31}$ – 275	$d_{31}$ – 920	$d_{32}$ – 1346
Piezoelectric voltage constant [ $10^{-3} \text{ V m N}^{-1}$ ]	$g_{31}$ – 9.5	$g_{31}$ – 17.1	$g_{32}$ – 24.9
Coercive field $E_c$ [kV cm <sup>-1</sup> ]	≈7.5	≈2.5	≈3.2
Curie temperature $T_c$ [°C]	320	145	160
Young's modulus [GPa]	$Y_{11}^E$ 61.0	$Y_{11}^E$ 19.8	$Y_{22}^E$ 22.93
Density [kg cm <sup>-3</sup> ]	7292	7986	8333

### 2.1.5. Single Crystals

Single crystal materials provide much better piezoelectric properties than the conventional PZT materials.<sup>[27]</sup> However, they are more expensive and thus seldom applied in the energy harvester. Lead magnesium niobate–lead titanate (PMN-PT), lead zirconate niobate–lead titanate (PZN-PT) are typical piezoelectric single crystal materials. To seek the potential, Z.G. Yang et al. investigated the performance of PZN-PT and PMN-PT in the applications of energy harvester and also compared with PZT.<sup>[28]</sup> Table 3 is the comparison of PZN-PT, PMN-PT, and PZT materials given by the authors. The single crystal materials as listed provide much larger  $d$  and  $g$  values and thus expected to have better energy-harvesting performance. Cantilever sample was used for the investigation. Both off-resonance and on-resonance condition was studied. In both cases, it can be seen that the single crystal samples generate more power and with higher efficiency than the PZT materials. This might prove that single crystal is a good choice energy-harvesting materials. However, potential problems of the crystal, such as fatigue, fabrication, cost, temperature, nonlinearity, etc. are indicated. Only the soft PZT material was studied, while the hard material is still an open question. Therefore, more research will be necessary to estimate the energy harvesting performance of the single crystal materials at various conditions.

### 2.1.6. Composites

The composite materials have been investigated for specific energy-harvesting applications. A strain energy harvester using the PZT–polymer composites was developed for tire applications, in which the strain –0.28% to 0.72% strain is required.<sup>[29]</sup> Noting that PZT materials may depole and fracture at high strain levels, while on contrast, PVDF polymer has higher tensile strain limit, but insufficient thermal properties for use in automobile tires. Therefore, compound of these two is expected to possess both adequate thermal and mechanical properties. Three samples were prepared by applying the mixture of PU and PZT5A4 powder. The first sample contains dispersed granular PZT particles. The second contains dielectrophoretic (DEP) processed PZT

particles and the last contains PZT fibers. The prepared samples were also compared with the counterpart PVDF and macrofiber composite (MFC). In terms of materials properties  $d_{ij}$ , the composite is one order lower than the PVDF or MFC samples, therefore accordingly the lower charge output. However, when considering the stability, the composites show advantages. The PVDF and MFC samples degrade irreversibly at elevated temperature conditions. On the contrary, even though, the performance of composites reduces also, but it is mainly due to glass transition of the PU phase and can be recovered. This property makes it more suitable for tire application than the PVDF and MFC counterpart. Therefore, besides the parameters in Equation (11), the stability and environmental conditions should also be in consideration. In practice, a balance between different parameters might be necessary.

### 2.1.7. Comparisons

Table 4 gives a summary of the materials described above, including the categories, representing materials, their advantages, disadvantages, and the recommended fields of applications. In general, the PZT ceramic is the benchmark; and other materials are more suitable for applications in a specific area or direction. Currently, many of the energy harvesters have been able to generate power over mW. In the future, to further improve the output performance, the material properties must be enhanced. In the short term, conventional methods, such as previously mentioned doping and microstructure modification might be necessary and recommended. And in the long run, new findings in the materials development may bring the breakthrough the energy harvesters.

## 2.2. Orientation of Materials

### 2.2.1. 31-Mode

The 31-mode is one of the mode common mode and the samples can be conveniently manufactured in various size and shape.<sup>[30]</sup> An example of 31-mode energy harvester is investigated in ref. [30a]. It consists of a piezoelectric patch and a brass or

**Table 4.** Comments and comparisons of different materials.

Materials	Examples	Advantages	Disadvantages	Application
Ceramics	PZT	Good piezoelectric, mechanical, and thermal properties; easy fabrication; easy shaping; good stability; low cost	Toxic lead	General applications
Polymers	PVDF	Good mechanical flexibilities; higher chemical resistance	One order lower piezoelectric coefficients than PZT; narrower working temperature range	Wearable; biocompatible
Lead-free	BT, BNT, KNN	Lead free; comparable piezoelectric properties with PZT in some composition	Overall lower piezoelectric properties than PZT; lower thermal stability; more difficulties in processing	Environmental compatible; general application
Nanomaterials	ZnO	Easy to form nano structures: no poling is required; chemically stable, biologically safe; low cost	Lower piezoelectric properties	Nanogenerator for consumable electronics
Single crystals	PMT-PT PZN-PT	Very good piezoelectric performance	Toxic lead; lower mechanical properties; higher cost; difficult to fabricate and process	General application
Composites	PZT + PVDF	Possibly to have advantages of both phases in the compounds	Complicated processing required	Special scenario like both flexibility and thermal properties are required

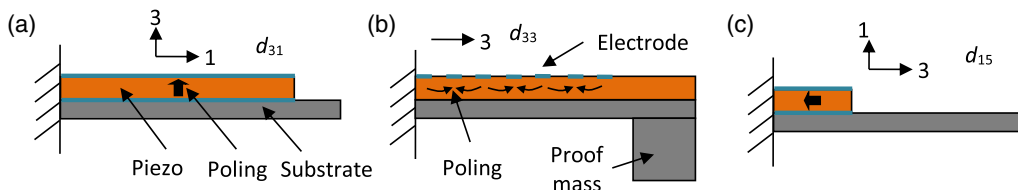


**Figure 2.** Typical orientations in the design of piezoelectric energy harvester: a) 31-mode, b) 33-mode, and c) 15-mode.

stainless steel substrate (**Figure 2a**). They are bonded together using epoxy. Theoretical modeling and structural optimization have been given and the output voltage, generated charges, and energy were studied. The thickness ratio and modulus ratio between the substrate and the piezoelectric layers are found to affect the output performances. By varying the thickness ratio only, the voltage peak will be observed. In contrast, when varying the modulus only, the voltage will increase first, then saturate. Another example of 31-mode cantilever unimorph-type energy harvester is presented in ref. [30b]. It is ZnO based with a tiny size of 3000 μm in length, 1500 μm in width, and 5 μm in thickness. The ZnO material is sandwiched between two metal electrodes. At the end of the cantilever, a 500 × 1500 × 380 μm<sup>3</sup> proof mass is added for the frequency tuning. The fabrication of device is based on the SOI bulk micromachining process. The characteristic of the harvester is that resonant frequency is 235.38 Hz, open-circuit peak-to-peak voltage is 306 mV at 0.1 g acceleration. This value is lower than that in ref. [30a], which is around 15 V<sub>pp</sub> at 2 g accelerations. However, in consideration of the smaller size (3000 μm vs 50 mm in total length) and the lower acceleration (0.1 g vs 2 g), the performance might be fair.

### 2.2.2. 33-Mode

As shown in Table 1, the value of  $d_{33}$  for PZT materials is more than twice that of  $d_{31}$ . Hence, 33-mode energy harvester is expected to have better performance than the 31-mode harvester. The 33-mode energy harvester have different designs.<sup>[31]</sup> A MEMS cantilever harvester has been studied in ref. [31a]. Its configuration can be illustrated in Figure 2b. To achieve the 33-mode, the interdigital electrodes were applied. After poling, the spontaneous polarization will be in-plane aligned with the PZT layer. The device is able to generate higher voltage than the 31-mode counterpart. This is due to a higher  $d$  coefficient value and the controlled capacitance which is done by adjusting the electrode gap. This is consistent with our previous analysis in Equation (11). The testing results show the device generates a power density of 7.3 mW cm<sup>-3</sup> g<sup>-2</sup>. The authors claimed that this is an extremely high power density at the very low acceleration of 0.39 g. Another 33-mode harvester based on piezoelectric stack is presented in ref. [31b]. The stack is formed by two PZT rings with opposite polarities. A metal sheet is inserted between the two PZT rings as the common electrode for delivering the output signal. The whole device has the stack-spring-mass-spring-stack structure. During operation, the device can be fixed to the shaker. The oscillation of the shaker will excite the mass and thus apply force on the PZT stack. The experimental results show that the harvester was able to generate open-circuit voltage more than

4 V<sub>p-p</sub> and around 0.9 μW powers at 5 g acceleration. The output of the device is also stable, at 9 g acceleration, over 12 h test, the output voltage almost has no change. The stack configuration is a typical structure of the piezoelectric devices. For many cases, they are in the form of multilayer stack. The poling direction is along the axis of the stack. Therefore, the force is along the 33 direction. Compared with the cantilever, this configuration is more suitable for large force excitations as it is more bulky than the cantilever.

### 2.2.3. 15-Mode

The 15-mode is the shear mode. The interests on 15-mode is because normally for PZT materials,  $d_{15}$  is larger than  $d_{33}$  and  $d_{31}$ . Hence, even the 15-mode sample is more difficult to be prepared, it still attracts many researchers.<sup>[32]</sup> Zhao et al. designed a 15-mode energy harvester that contains two PZT elements in 15-mode, and they are connected in series to improve the voltage output.<sup>[32a]</sup> The material is PZT-51, which  $d_{15}$  is  $700 \times 10^{-12}$  CN<sup>-1</sup>,  $d_{33}$  is  $460 \times 10^{-12}$  CN<sup>-1</sup>, and  $d_{31}$  is  $-190 \times 10^{-12}$  CN<sup>-1</sup>, respectively. The structure of the device is shown in Figure 2c. Single piezoelectric element design and two elements in series design are studied and compared. There is no comparison of the device with 33- and 31-mode harvesters. However, a useful conclusion about this work is that the series connection can improve the energy harvesting performance for the 15-mode piezoelectric energy harvester compared with the single element one. The transient voltage was improved from 15.6 to 25.4 V<sub>pp</sub> at resonance. This result is interesting and indicates that the structure design shall be included in the design consideration for the improvement. This concept will be introduced in the next section. Another design of 15-mode energy harvester is shown in ref. [32b]. In this design, the single-crystal PIN-PMN-PT material was applied. The energy harvester contains two pieces of the crystals in the series connection. The crystals were sandwiched between a top beryllium copper bridge and a bottom PMMA substrate. A cubic copper proof mass was also applied on the top of the bridge. When the device is accelerated, the bridge transfers the force from the normal direction to the direction parallel to the surface of the crystal, as a result, generating the 15-mode of the crystal materials. The advantages of the design is the large figure-of-merit  $d_{15} \times g_{15}$  ( $1.296 \times 10^{-10}$  CV mN<sup>-2</sup>). As the results, the harvester achieved a maximum power density of  $1.378 \times 10^4$  Wm<sup>-3</sup>, which is 5.5 times higher than the same structured energy harvester made from soft piezoelectric ceramics. However, the resonant frequency of the harvester is pretty high around 1000 Hz, which is out of the range of many excitation sources.

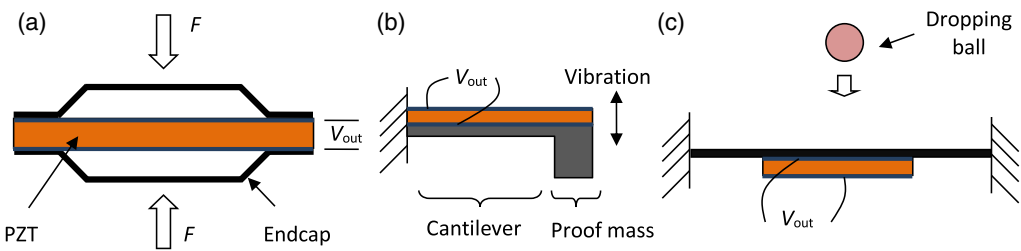


**Figure 3.** Typical structural design of piezoelectric energy harvester a) off-resonance cymbal transducer, b) resonance  $d_{33}$  cantilever harvester, and c) dropping ball impact generator.

### 3. Structure Designs

As analyzed in the previous introduction, the structure is another important group of parameters that contributes the output performance of the energy harvester significantly. The structure parameters shall include dimensions and configurations. They affect both mechanical and electrical properties. There are many structure designs in the literature. In general, they can be classified as off-resonance, on-resonance, and impact design. To be noted that many structures can apply both in off-resonance, and on-resonance or even impact designs.

#### 3.1. Off-Resonance Design

In off-resonance design, a low-frequency cyclic or slow varying load is applied to the energy harvester, and it is usually below the resonance frequency. An example of off-resonance design is presented in ref. [33], which is a piezoelectric cymbal transducer with configuration as shown in Figure 3a. It mainly consists of a PZT disk sandwiched between two metal endcaps. The energy harvester is targeted at gait analysis (2 Hz as reference). Therefore, it can be considered as an off-resonance energy harvester. For off-resonance design, other than the materials, the structural configurations are one of focusing point for the improvement of output performance. Regarding this cymbal, the key configuration is the two endcaps which works as the amplifier, and is considered to be able to amplify the force exerted on the PZT disk, as a result, improve the performance. Therefore, the dimension of the endcap, including, thickness, joint length, and angles etc have been optimized. As the result, the obtained harvester with dimension  $\phi 30 \times 4.6$  mm, thickness 0.33 mm was able to harvest 1.2 mW power under a 50 N force at 2 Hz and  $10\text{ M}\Omega$  optimal resistor load. Another cymbal harvester made with ceramic diameter 29 mm and optimal thickness of 1 mm, under AC force of 70 N and prestress load 67 N, at 100 Hz, 52 mW powers was obtained across a  $400\text{ k}\Omega$  resistor.<sup>[34]</sup> There is a large increase of the power output compared with the previous example. One of the reasons could be the increased frequency from 2 to 100 Hz. So even in off-resonance design, frequency is also an important parameter and should not be neglected.

There are also some other means applied in the structural design, for example multilayered stack,<sup>[35]</sup> prestressed and curved thunder,<sup>[36]</sup> parallel arranged piezoelectric links,<sup>[37]</sup> and so on. More or less, for those designs, there is amplification

**Table 5.** Frequency and acceleration of various vibration sources.<sup>[38]</sup>

Vibration source	Frequency [Hz]	Acceleration amplitude [ $\text{m s}^{-2}$ ]
Car Instrument panel	13	3
Casing of kitchen blender	121	6.4
Clothe dryer	121	3.5
HV AC vents in office building	60	0.2–1.5
Car engine compartment	200	12
Refrigerator	240	0.1
Human walking	2–3	2–3

mechanism in the devices. Modifications are made on the effective material parameters, enlarge the force acting the function materials, accumulate the energy from multiple samples, extend the device safe operation range, optimize the stress distribution, and so on. Those mechanisms may suit both off- and on-resonance conditions.

#### 3.2. Resonance Design

In some specific situations, the frequency range is clearly known in a certain range during application as listed in Table 5.<sup>[38]</sup> For those situations, tuning the frequency to the resonance will be of great of advantages for the power output. The cantilever + proof mass design, as shown in Figure 3b, is a widely applied structure for the resonance energy harvester. The cantilever is fixed at one end, and the other end is designed with a proof mass. The frequency can be adjusted through the cantilever length, thickness, and proof mass.

A MEMS cantilever energy harvester is developed in ref. [39]. The 33-mode design was applied in the devices, and a 20 times or greater output is realized. The cantilever device was fabricated using three photo mask process. After fabrication, the device is shown the bow curvature, which can be minimized through the optimization of the fabrication process. The resonant frequency is 13.9 kHz, which is fairly high for an energy harvester as compared in the Table 5. And finally, a  $170 \times 260 \mu\text{m}^2$  PZT harvester could generate  $2.4\text{ V}_{dc}$  and  $1\text{ }\mu\text{W}$  power at 5.2 MG resistive load. The energy density is  $0.74\text{ mWh cm}^{-2}$ . The author claims it compares favorably to the values of lithium ion batteries. The author expects to reduce the frequency, while obtain enough energy in next generation of device.

The concept of cantilever and proof mass works well. However, there are also many modifications for the further improvement, for example, Lee et al. presents a hybrid design, in which the electromagnetic mechanism was also included.<sup>[40]</sup> A multiband design, in which rotational cylinder was used as proof mass is shown in ref. [41]; and ref. [42] presents a wide-band design, in which the seesaw mechanism was applied. In most cases, these harvesters use the bending vibration mode, as this mode is much easier to be tuned to a low frequency.

### 3.3. Impact Design

In the impact design, the energy harvester is exerted with an impulse force. An example is shown by Umeda et al. in ref. [43]. The concept is illustrated in Figure 3c. It consists of a steel ball and a piezoelectric unimorph vibrator. The steel ball falls freely and impacts the center of the vibrator. The vibrator then responds dynamically. The output will be supplied to a load resistor. The waveform across the load contains two parts: immediately after impact with low frequency components and following decaying oscillation with high-frequency components. Around 10% maximum efficiency was observed. By modeling, it can be concluded that the efficiency increases when  $Q_m$  increases,  $k^2$  increase, and  $\tan\delta$  decreases. This conclusion supports the previous Equation (11) and (12). There are a few more research on impact designs which will be discussed in the later part of impact force. It will be seen that the impact design is more suitable for high voltage generator.

## 4. Forces and Excitations

Forces acting on the harvester are important considerations when designing the energy harvesters. Different types of forces have features in regard to the magnitude, frequency, speed, directions, period, and etc. Various sources of forces and excitations have been studied. In this section, we will focus on the sources of different forces and their general features.

### 4.1. Excitations from Direct Contact Force

For off-resonance energy harvester, a direct contact force excitation acting on a segment of the harvester is quite normal. The force usually might be low and intermediate speed, periodic, or random. An example of such force of excitation is an energy-harvesting mat.<sup>[44]</sup> The prototype consists of 16 piezoelectric transducers under a rubber mat. A few tests were carried out, in which students perform walking, jogging, squatting, lunging, and sit-up. The voltage is about a few volts as obtained from the published data plot. The contact areas and speed affect the voltage with more significance as the body weight is acting as the main forces of excitations. It was documented that during walking, the reaction force may rise to 1.5 times of the body weight, and during running, it is 2–2.9 times of the body weight.<sup>[45]</sup> And according to ref. [46], the force profile for a moderately paced walking step is characterized by a double peak at  $\approx 1.2$  times the body weight, occurring as a result of heel strike and forefoot push-off. This indicates that different activities of the human

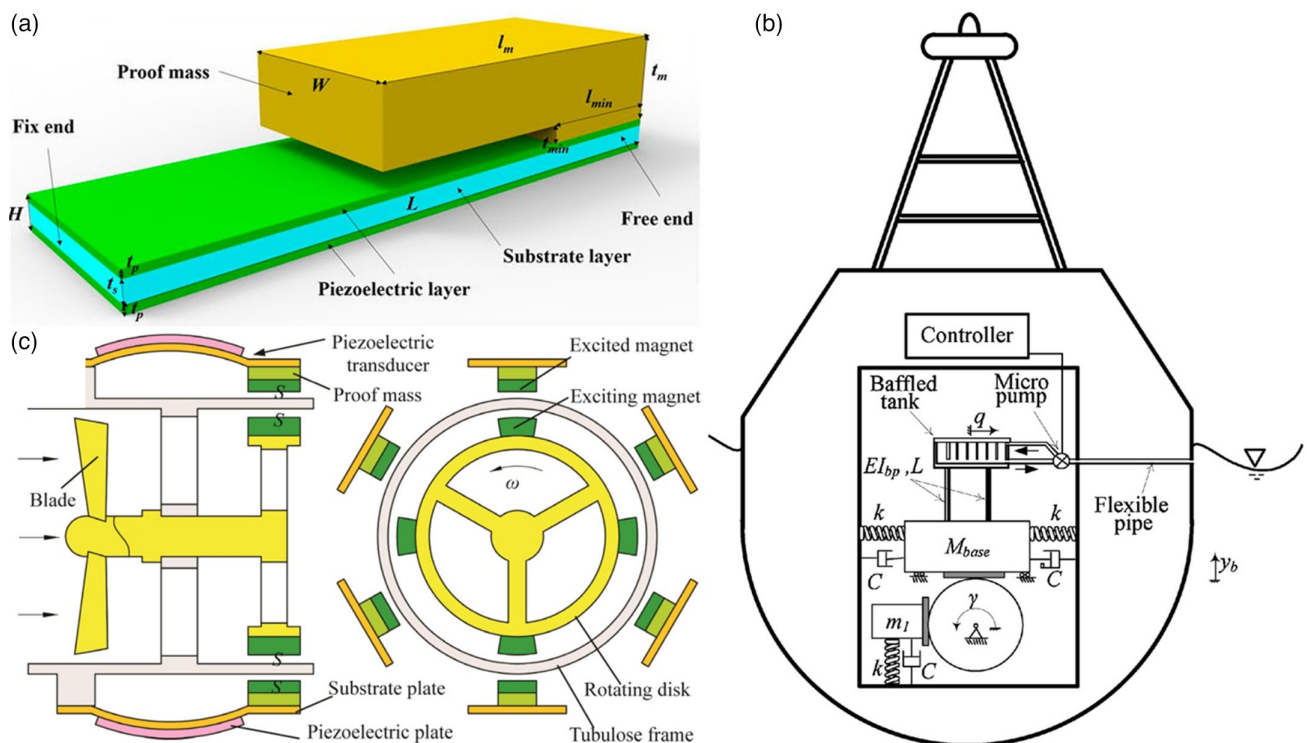


**Figure 4.** Typical energy harvesters with different excitation sources. a) Bimorph cantilevers with L type mass. Reproduced with permission.<sup>[47]</sup> Copyright 2018, AIP Publishing LLC. b) Concept of the buoy. Reproduced with permission.<sup>[49]</sup> Copyright 2018, Elsevier. c) The wind-mill. Reproduced with permission.<sup>[50]</sup> Copyright 2016, Elsevier.

body will induce different magnitudes and profile of forces, as a result of different voltages.

#### 4.2. Excitation from Low Vibrations

The vibration-type energy harvester is a larger category of energy harvester. The vibrations sources come from various machineries or structures. Some examples have been illustrated previously in Table 4. This type of energy harvester, mostly adopts the architecture of cantilever and proof mass. The vibration source generates an inertial force and applied to the harvester which responds dynamically. Typically, the harvester produces maximum power at the resonance frequency. Designing low resonance harvester is of main interest, as shown in Figure 4a of a novel L shape proof mass.<sup>[47]</sup> The harvester was excited with a shaker and with resonant frequency of 18.1 Hz, lower than many harvesters in the literature. The power output of 192 mW g<sup>-2</sup> can be obtained at the resonance. The corresponding power density is 24.6 mW (cm<sup>3</sup>g<sup>-2</sup>)<sup>-1</sup>.

#### 4.3. Excitation from Hydraulic and Pneumatic Power

Some efforts have been made in utilizing the fluid dynamics as the energy-harvesting source. An eel-type energy harvester was developed which converts mechanical energy in ocean or river water flows into electricity.<sup>[48]</sup> The device consists of a bluff body and a long strip of piezoelectric polymers. In a nonturbulent flow, the bluff body regularly sheds alternating vortices on either side of the bluff body. The resulting pressure difference forces the polymer strip to move in an oscillating motion like the eel swimming. The advantage of the harvester is that the piezoelectric polymer can be easily scalable in size and have a capacity to generate power from mW to W depending on the system size and flow velocity. The authors studied a few flow velocities of 0.35, 0.5, and 0.67 m s<sup>-1</sup>. The frequency of eel motion is in the order of 1 Hz and output power increases with the flow velocity.

Figure 4b presents another energy harvester using the ocean wave.<sup>[49]</sup> It is essentially a cantilever and proof mass system installed on an offshore buoy. The mechanical energy generated by the wave motion is transferred to the cantilever and proof mass system by a series of mechanical design. The natural frequency of the harvester can be tuned close to ocean wave frequency which is in the order of 1 rad s<sup>-1</sup>. Around 10 mW power can be obtained. The authors claim that a few such harvesters will be sufficient for powering the sensors in the buoy.

The above two examples show the liquid flow energy. Even though the frequency is low, it is continuous and as a result not-stop power generation becomes possible, which is difficult to achieve for many mechanical sources. The time accumulation is important as shown in the previous analysis in Equation (11). Furthermore, large-scale harvester is possible for such energy sources.

Another example of using the fluidic force is the wind driving energy harvester, as shown in Figure 4c.<sup>[50]</sup> The cantilever and proof mass structure is applied as the energy-harvesting structure. The constant velocity wind flow is converted to a periodical magnetic force through the fan blade mechanism and repulsively applied to the proof mass. The output of the energy is affected by the number of magnets and wind velocities. Multiple optimal

values are shown in the velocity–output spectrum depending on the number of magnets. Within the reported experimental range, a maximum voltage of 37.2 V and energy of 2.24 mJ was observed.

#### 4.4. Excitations from Acoustic Wave

A piezoelectric MEMS energy harvester is introduced in ref. [51]. It has a squared daisy structure with central mass and vibration enhancement petal cantilevers. In operation, the acoustic waves will induce mechanical vibration, which in turn converted into the electricity based on the piezoelectric transducer 31-mode. The daisy harvester was tested using a speaker at a certain distance and up to 22 kHz. The results show that at a so-called minimal test distance 0.92 mm, power up to 16 nW, and 30.5 mV can be obtained. The power reduces as the distance increases, but there may exist local maximum at half wavelength. The acoustic energy harvester is a noncontact means for energy harvesting, however as illustrated the power is in the nW range. The previous example of using the magnetic force is also an example of non-contact force.

### 5. Frequency and Speed

In general, higher speed and frequency are advantageous for energy harvesting. Even though high speed and frequency citation are not typical in the nature, they are still attractive to many applications. The following section gives some examples.

#### 5.1. High Speed and High Impact

The impact force can be large in magnitude and fast in speed. In this type of energy harvester, a moving object is usually applied to hit the static piezoelectric transducer to generate energy. Most of such energy harvester is for repetitive usage; however, a few cases are only for one time application.

Another falling ball impact power generator is illustrated in ref. [52]. Different from previous example in ref. [43], the series amplification mechanism was applied to increase the voltage as much as three times. The test results showed that under the impact from 1 to 5 MPa, the peak output voltage can be increased from 100 to 900 V. This is quite a high voltage compared with many other energy harvesters.

The igniter is a piezoelectric example that is used in the mainstream of ignition sources for gas apparatus.<sup>[53]</sup> The high mechanical stress that impacts the piezoelectric element of typically 3 mm in diameter and 5 mm in length with high  $k_{33}$ ,  $g_{33}$ , and coercive force could generate high discharge energy. Usually, a 10–20 kV voltage under a 200–500 kG cm<sup>-2</sup> mechanical stress is generated.

The ferroelectric generator is a good example of using high impact force and fast impact speed.<sup>[54]</sup> The mechanism of ferroelectric generator is based on the high charge density (30  $\mu$ C cm<sup>-2</sup>) high electromagnetic energy density (4 J cm<sup>-3</sup>) of PZT ceramics after poling.<sup>[54a]</sup> A quick release of such energy in the order of microseconds will generate high power, high voltage and high current. To initiate such process, in practice, the explosive energy is used, which accelerates an impactor, hitting

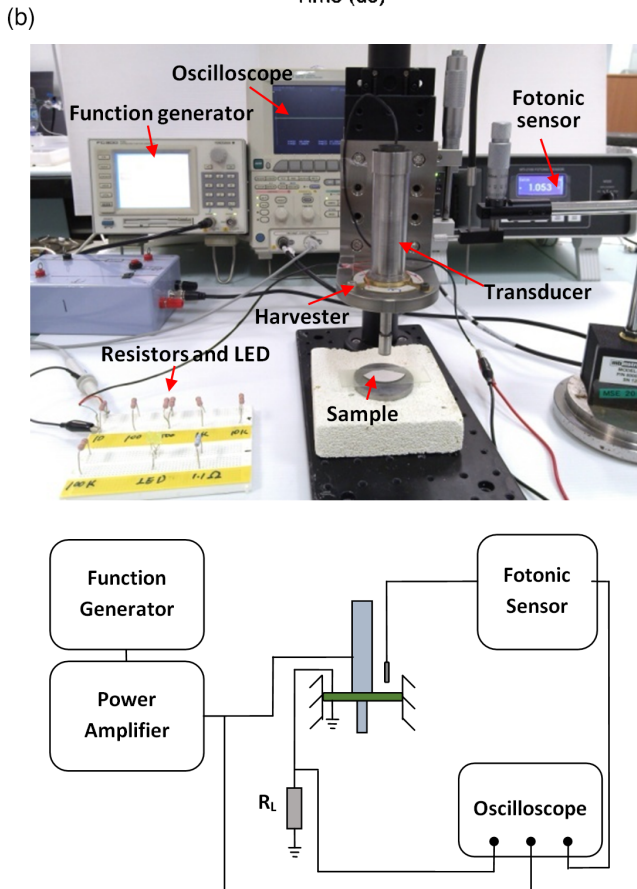
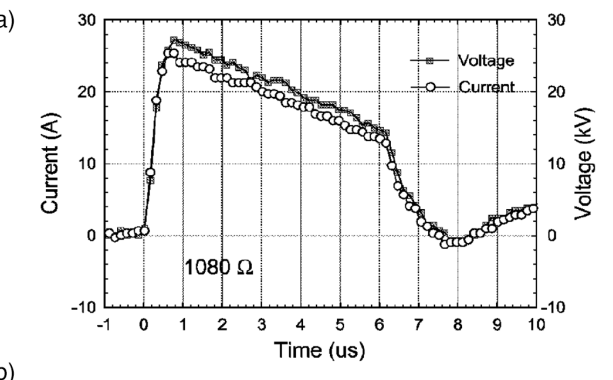


**Figure 5.** Examples and performances of high impact and high-frequency designs. a) Current and voltage waveform under 12 GPa and 1080  $\Omega$  load resistance. Reproduced with permission.<sup>[54b]</sup> Copyright 2004, AIP Publishing LLC. b) Ultrasonic energy harvester and test system. Reproduced with permission.<sup>[2]</sup> Copyright 2019, MDPI.

on the PZT ceramics to generate the shock wave. Due to the high impact stress, the sample will eventually be depoled and destroyed. Meanwhile large energy is released. An example of output is shown in the **Figure 5a**. The peak current is 26 A and 27 kV, respectively. These values are extremely high compared with the other current piezoelectric energy-harvesting technologies. However, the process is not reversible. Therefore, the potential application is also narrower than its counterpart.

## 5.2. High-Frequency Ultrasonic Vibration

The ultrasonic devices are widely applied in the industries, for example, ultrasonic cleaner in the wet lab, ultrasonic probe in the chemistry field, ultrasonic welding, cutting in the advanced manufacturing, ultrasonic transducer in the underwater communications, and so on. Those devices usually work in the frequency above 20 kHz to tens of MHz. The frequency is extremely high compared with the normally applied low-frequency harvesters. We have reported the use of ultrasonic technology for high-frequency energy harvesting.<sup>[2]</sup> A theoretical model was provided, and an experimental prototype was fabricated. From the model, the maximum power output is expressed as

$$P = \frac{\omega Q^2}{2C} \quad (13)$$

This expression is actually consistent with the relation given in refs. [4a,20,55] that shows higher frequency brings higher power output. Some other relations, for example voltage and current in relations to the frequency, were also provided.

A harvester device was developed and integrated to an ultrasonic cutting transducer, as shown in Figure 5b. The device is a circular unimorph, one end is connected to the transducer, the other end to the fixture. When the transducer vibrates, the leak vibration from the transducer will energize the harvesters. The operating frequency of harvester is 24.4 kHz. Two unique features were identified: high current generation capability (20 mA<sub>pp</sub> in the testing condition) and low impedance matching resistance (500  $\Omega$  in the testing condition). Ultrasonic energy harvester so far is not a mainstream in the research field. However, it deserves more investigations as it provides a new direction for energy harvesting. Other examples include those reported in ref. [56].

## 6. Electrical Load

The energy harvester will eventually deliver the energy to the followed electrical devices in the next stage of the system, for example sensors, microcontrollers, transmitters, and so on. In general, those devices can be approximated as the electrical resistive load to the energy harvester. The relations between the output from the energy harvester and the resistive load have been investigated intensively by many researchers.<sup>[2,57]</sup> A summary of output performance, such as voltage, current, and power as a function of external load resistance are shown in **Figure 6**.<sup>[2]</sup> In general, across the load resistance, the voltage increases then saturates, the current decrease gradually, and the power will show peak value. This variation can be theoretically deduced from the Equation (5)–(7) in the earlier sections. Some experimental validation can also be found in ref. [57a]. Compared with Figure 6, consistent voltage, power profile in relation to the load resistance was experimentally observed.

There are a few things that shall be known regarding the electrical load. First, the output of the energy harvester is always random, nonconstant, and intermittent. So usually, the energy

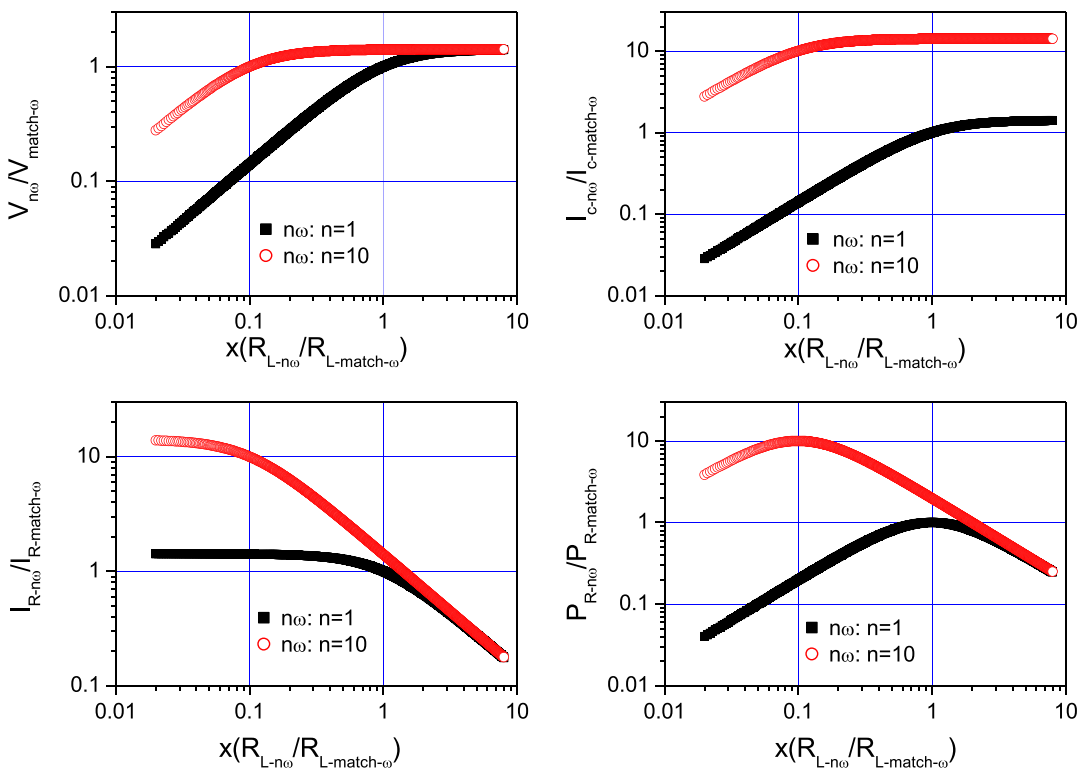


**Figure 6.** Output performance as a function of load resistance. Reproduced with permission.<sup>[2]</sup> Copyright 2019, MDPI.

harvester will not be directly connected to the electrical device. There is a power management circuit, providing functions, such as AC–DC conversion, energy storage, output control, impedance matching, and so on. For example, LTC3588 power management circuit was integrated in the energy harvester for stabilizing the voltage output in ref. [57b]. Second, the impedance matching is an important consideration in energy harvesters. From ref. [2], the matching resistance is  $1/\omega C$ , where the output power reaches the maximum value (Equation (13), Figure 6). Some power management circuit has been investigated for better impedance matching. For example, an adaptive impedance matching circuit was presented in ref. [57c]. The circuit mainly consists of a full bridge rectifier, a buck-boost circuit, a peak detection module and a controller. When the piezoelectric harvester is undergoing impact excitation, the circuit is able to tune the self impedance according to the impact and vibration stage. Experimental results showed that the efficiency of the circuit was able to reach 80%, 18% higher than the conventional rectifier circuit. Third, the piezoelectric energy harvester is usually high impedance output devices due to the low frequency and small size operations. Thus, to achieve the high power output, transfer the energy effectively, or better impedance matching, the load resistance is usually high. However, as frequency increases, this property will be modified as indicated in Equation (13). This has been analyzed in ref.[2] in detail, where the high-frequency harvester shows lower impedance matching resistance and larger current generation capability.

## 7. Time and Accumulation

The last item in Equation (11) is time. It essentially indicates that the accumulating effect, i.e., the total generated energy increases with time. Generally, an energy harvester scavenges minute energy from the environment in an intermittent way, the instantaneous power may not be sufficient for practical application. Hence, many researchers consider time accumulation of the energy through means like a super capacitor or batteries. A system was applied in ref.[58] that consists of an energy harvester, a bridge rectifier, a filter capacitor, a switch, a controller, and a battery. The system works in two stages: first, the transient charging, in which the filter capacitor is charged; then, the steady-state charging, in which the switch is closed, and the battery is charged. The controller triggers the on/off state of the switch according to the voltage across the filter capacitor. The system was tested. The transient charging of the filter capacitor is successful. The voltage increases with a fast speed. However, only theoretical values of the steady-stage charging were provided. According to the author, higher efficiency circuit shall be developed. Capacitor charging can also be found in some other references with a certain degree of success.<sup>[13,59]</sup>

The feasibility of charging batteries has been examined in ref. [60] using the PZT and MFC that were fabricated into the unimorph structure and tested as the cantilever harvester on a shaker. The MFC is identified less efficient than PZT due to the less current generation. Therefore, PZT harvester is applied

to charge the NiMH with different capacities. Two conditions, resonance at 50 Hz and random at 0–500 Hz, was tested. As the battery capacity increases, the charging time increases also. Future work may include the optimization of the charging circuit for constant power supply.

## 8. Applications

Energy matching to a specific application is an important topic of energy harvesters. From the literature, potential applications ranging from consumer electronics, to industrial equipments and military usages, have been explored. Some of the examples are introduced below.

### 8.1. Structural Health Monitoring

Upon long time or harsh environment operations, damages may appear in the civil or engineering structures. Therefore, to ensure the safety and reliability of the structure, constant monitoring, fault detection followed by timely repair are important and necessary. This typically involves advanced monitoring techniques, such as sensors and sensor networks. However, large area deployment of the sensors may incur maintenance problems, for example, high-cost replacement of the power sources in the inaccessible locations. Therefore, interests on self-powered structural health monitoring devices arise.<sup>[59]</sup> The competitive advantage of piezoelectric energy harvester in this area is that the piezoelectric device can work both as sensors and energy harvesters. As the energy harvester, it produces energy from the structure vibration, wind flows, or the structure deformations. As the sensor, it could measure the external parameters, such as strain, acceleration, or sound waves pressures. The piezoelectric energy harvester can be applied both on civil structures, such as building, or engineering structures, such as aircraft. Research efforts aiming at powerless sensing technique have been carried out.

The application of energy harvesters on civil structures in smart city and structural health monitoring has been highlighted in ref. [59b]. Some challenges include the frequency mismatch between the energy harvester and the civil structure, and the random vibration signals of the civil structure. Measurement of the frequency of a flyover, typically 5 Hz was obtained, and a lab test shows the 0.2  $\mu$ W power can be generated with a cantilever harvester, and a capacitor can be charged to 1.2 V within a few second.

An embedded self-powered strain sensing system (SES) for structure damage detections was prepared in ref. [59a]. The sensor is made of PVDF, which generates energy under mechanical stress. The energy is first stored in a capacitor, and then supplied to a RF transmitter for signal transmission. The device is applied for damage detection. The signals within 1 m were successfully detected. The work demonstrates the feasibility for structural health monitoring with self-powered wireless sensors.

An algorithm was proposed to improve the performance of the piezoelectric energy harvester.<sup>[59d]</sup> This algorithm is based on the topology optimization of the structure design. For aircraft structure applications, the frequency is in the range of 100–500 Hz. For such wide frequency range applications, wide band energy harvester is necessary. For the conventional approach, multiple

pieces of cantilever energy harvester with different resonant frequency have to be applied. For the algorithm of topology optimization, the shape of cantilever which consists of steel substrate and piezoelectric materials was optimized. The shape can be complicated. However, the frequencies of the first three harmonic vibrations modes fall exactly in the range of interest 100–500 Hz. Therefore, the purpose of wide band energy harvester can be achieved.

The possibility of leakage and damage of pipelines was exploited in ref. [59e]. The PVDF piezoelectric energy harvester was used as the strain sensor. The sensor is attached to the surface of the pipeline in parallel with a conventional strain gauge sensor for the purpose of validation. After calibration, the signals from the piezoelectric energy harvester and strain gauge sensor were compared. The good correlation between the healthy pipe and strain response can be deduced from the validation results. Therefore, the author concluded that the signals from the energy harvester are reliable and can be adopted for pipeline health analysis.

Another effort regarding the admittance method in aerospace structural health monitoring is shown in ref. [59f]. The PZT patch was attached to the mechanical structure. The energy is harvested from the flow-induced structural vibrations. The impedance from the piezoelectric patch was measured as a function of frequency. It can be found that the imaginary part of the admittance, i.e., the susceptance is sensitive to the damage of the system. The difference of the susceptance with its original value reflects the type of errors. The advantages of this method are that not only the damage detection, but also the sensor self-diagnosis and energy harvesting can be realized within the same system.

A typical self-powered engine health monitoring system was presented in ref. [59g]. The system consists of a vibration sensor node and a PC terminal. The data transmission between them is wireless. The sensor node is based on an accelerometer. An L-shaped wide band piezoelectric energy harvester was developed to power the sensor node. The node also contains power management circuit, power storage device, MCU, and antenna. The sensor node was attached to the automobile engine and then the vibration signal was measured. From the PC end, the data was analyzed. The abnormal data could be identified from the frequency spectrum. The measured signal can be used as an effective basis for engine structural health monitoring.

### 8.2. Engine Vibrations

Vibration harvesting from engine vibrations was demonstrated with a cantilever harvester with 155 mm length that was installed on the vehicle engine and tested in various engine speeds.<sup>[61]</sup> The system is shown in Figure 7a. It is found that in frequency match condition of around 2000 rpm engine speed, more energy can be harvested. The energy could be used for charging and discharging a capacitor. At the end of 8 S, a power of 0.177 mW can be obtained. As the engine speed is not constant, a wide band harvester might be considered in the future.

### 8.3. Gait Power for Personal Health Care

An application of shoe midsole energy harvester as medical devices is shown in ref. [46]. The motivation is to augment charging of

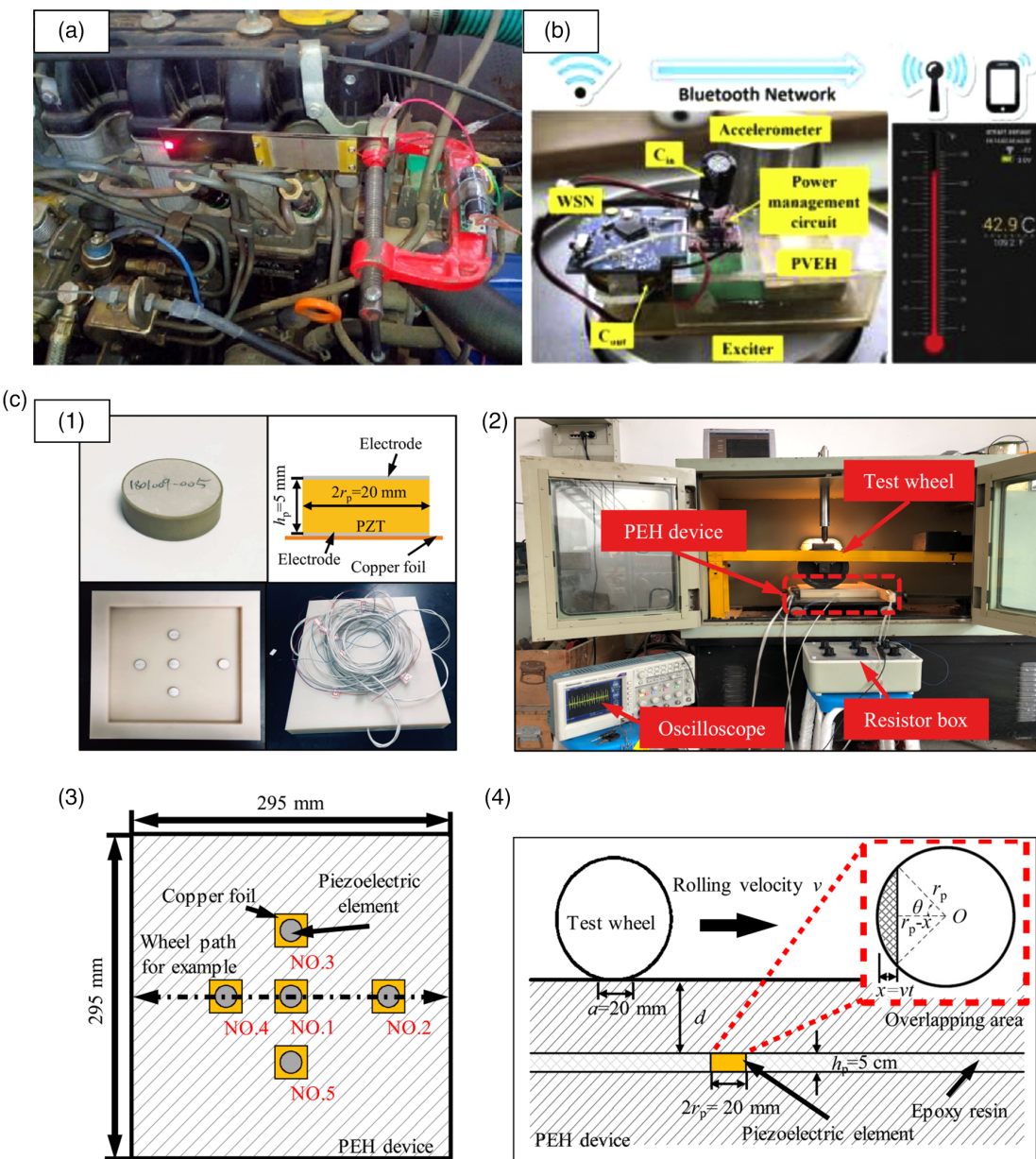


**Figure 7.** Examples of some applications. a) A cantilever harvester beam mounted on the engine. Reproduced with permission.<sup>[61]</sup> Copyright 2017, AIP Publishing LLC. b) Self-powered wireless sensor system. Reproduced with permission.<sup>[59c]</sup> Copyright 2020, Elsevier. c) The system of damage detection. Reproduced with permission.<sup>[65]</sup> Copyright 2019, ASME.

the internal batteries of the implanted device, for example ventricular assist devices, which typically draws energy 7 and 13 W, thus untethering the patient from external power for extended periods of time. Ground reaction force was identified to represent the greatest potential for usable energy. In theory, the instantaneous power levels as high as 100 W can be obtained, corresponding to total mean power of 8.2 W per foot under moderate gait ( $1 \text{ step s}^{-1}$ ). An energy harvester prototype was also designed, consisting of the PZT cylinder as harvester materials and the hydraulic amplifiers. A 1/17 scale model midsole generator was also tested. The result shows that  $5.7 \pm 2.2$  and  $23.6 \pm 11.6 \text{ mW kg}^{-1}$  powers for walking

and jogging can be obtained, respectively, indicating that for a 75 kg subject operating a pair of full size midsole generator, about 6.2 W power can be generated. The result looks positive. Further development and confirmation of an improved full-scale prototype might be necessary.

Zhou, et al. also presents an 3D-printed piezoelectric energy harvester for gait analysis.<sup>[62]</sup> The devices are using materials of BaTiO<sub>3</sub>-enhanced PVDF polymers with the kirigami structure. The device is stretchable up to strain 300% and can be mounted into wearable textiles, such as sock gait sensor and harvester. The generated voltage is about 6 V and current density is about

$2 \mu\text{A cm}^{-2}$ . The maximum power density is about  $1.4 \mu\text{W cm}^{-2}$  at  $10^7 \Omega$ . Some other shoe harvesters also exist in the literature.<sup>[63]</sup>

#### 8.4. Wireless Sensor Node

A design of wireless sensor node powered by the piezoelectric vibrating harvester for internet of things (IoTs) is shown in Figure 7b for wireless sensor node (WSN).<sup>[59c]</sup> The sensing system consists of a bimorph PZT energy harvester, a temperature sensor node, and a power management circuit. The harvested energy is first stored in a capacitor, then supplied to the rest part of the device for measurement and data transmission. Both theoretical analysis and experimental verification were carried out. The harvester resonant frequency is 22.3 Hz. Under 0.5 g excitation, the temperature was successfully measured, the average charging power is 1.28 mW, and charging time of 26 s.

#### 8.5. Military

Piezoelectric energy generator for gun-fired munitions and other similar applications that require very high acceleration G survivability can be achieved as shown in ref. [64]. It mainly consists of the spring-mass and piezo stack elements. The piezoelectric harvester harvests energy from the firing acceleration as well as the vibratory motion from flight. The developed generators are expected to withstand firing accelerations of over 100 000 Gs and provide over 2 J of electrical energy. The energy can be supplied for applications such as fuzing. Prototypes of a number designs have been successfully tested in the laboratory and by the USA Army using air guns.

#### 8.6. Pavement Power Generator

Using piezoelectric materials for pavement road power generators have been shown in ref. [65] and illustrated in Figure 7c. PZT materials were packaged using MC nylon and epoxy resin. The wheel rolling test was carried out. The wheel pressure is  $\approx 0.7 \text{ MPa}$ , and frequency 0.36 Hz. From the data plot, the voltage output is in the order of 10 V and power 1  $\mu\text{W}$ . The embedded depth was found to affect the power output, the deeper of the depth, the smaller of the power output. A scaling law was also provided for practical pavement harvester designs.

### 9. Future Prospects

The emergence of the energy-harvesting technology stems from the need of green energy and environment protection. Albeit the challenges met in wide adoption of mechanical energy harvesting, the demands on energy-harvesting technology will remain high. Identifying the capability of the energy harvesting in practical situations and matching the requirement of suitable applications serve as the key for adoption. To boost the progression of piezoelectric energy harvesters, the following efforts require attention 1) New materials development. The energy output will eventually depend on the materials itself with important considerations on the performance, size, and cost of the materials.

Many of the current piezoelectric energy harvesters have been able to generate power in the order of mW. However, it may not be continuous, and the current output is generally low, thereby limiting the power output. Developing materials that generate moderate voltage, higher current (requiring higher piezoelectric constant), and with acceptable scalability and manufacturability are desirable. Furthermore, to be comparable with other technologies for example solar cell, the cost shall be low enough. 2) Low power all-in-one device. It has been claimed that the current energy harvester is able to power many micro devices, for example, multiple sensors. Modern devices are increasingly complicated and may contain several or numerous components or modules to complete the full functionality. Thus, it is desirable that the energy harvester is able to supply sufficient energy to the whole arrays of devices. Therefore, the development of tiny all-in-one electrical device with small power consumption, such as sensor node, is necessary for the quick adoption of the energy harvesters. 3) Niche market application. Even though there exist limitations in current technology in catering for wide range applications, there are niche market which remain attractive. For example, the gas igniter has been very successful. Exploring the possible applications and market are also one of the important tasks for the future of the energy harvesters. Possible directions might include harsh environment, inaccessible locations, emergency situations, extreme conditions, military applications and so on. We have earlier demonstrated an ultrasonic energy harvester in ref. [2], which harvests energy from the high-power ultrasonic device with advantages of higher current generation capability and lower impedance matching resistance. The application falls in the niche area of engineering structural health monitoring. Other promising fields were also proposed in ref. [21b], for example, IoTs, consumer electronics, wearable sensor, and so on.

### 10. Conclusion

According to the derived theoretical model, the performance of the piezoelectric energy harvesting is related to a few groups of parameters, comprising of materials, structures, excitations, electrical load, frequency/speed, and time. Ceramics, polymers, single crystals, composites, nanomaterials, and lead-free materials have been widely applied as piezoelectric energy harvesters, with PZT as the benchmark material. Some materials have been found to be better than PZT in certain specific aspects. The parameter of DFOM could be used to estimate the competitiveness of the materials candidate. Regarding the structures, typically, there are the off-resonance, on-resonance and impact designs. The cantilever and proof mass structure are well-accepted resonance designs. While the force and excitations sources are diverse, the direct contact force, low vibration force, hydraulic, pneumatic power, and acoustic power can be frequently observed elsewhere. High-frequency and high-speed harvester are not very common; however, they may provide superior properties in some aspects. The factors of electrical load, impedance matching shall be considered for the design of piezoelectric harvester. Lastly, accumulation of energy with time is important for practical applications such as through capacitor charging.

Energy harvesters have many potential applications ranging from personal consumables to sustainable smart cities. In the future, materials optimization and discoveries, low power device design, energy source exploration, energy output maximization, and application matching are the important tasks to fully harness the potential of piezoelectrics as sustainable energy sources.

## Acknowledgements

This work was supported by the National Research Foundation, Prime Minister's Office, Singapore, under its Campus for Research Excellence and Technological Enterprise (CREATE) program.

## Conflict of Interest

The authors declare no conflict of interest.

## Keywords

energy harvesters, nanogenerators, piezoelectrics, power generators, scavengers

Received: July 29, 2021

Revised: November 30, 2021

Published online: January 6, 2022

- [1] a) L. Zuo, X. D. Tang, *J. Intell. Mater. Syst. Struct.* **2013**, *24*, 1405; b) S. R. Anton, H. A. Sodano, *Smart Mater. Struct.* **2007**, *16*, R1; c) M. R. Sarker, S. Julai, M. F. M. Sabri, S. M. Said, M. M. Islam, M. Tahir, *Sens. Actuators A* **2019**, *300*, 111634.
- [2] T. Li, P. S. Lee, *Actuators* **2019**, *8*, 8.
- [3] a) M. Prauzek, J. Konecny, M. Borova, K. Janosova, J. Hlavica, P. Musilek, *Sensors* **2018**, *18*, 2446; b) J. D. Song, J. Wang, *Sci. China Tech. Sci.* **2016**, *59*, 1012; c) S. G. Kim, S. Priya, I. Kanno, *Phys. Conf. Ser.* **2015**, *660*, 012001.
- [4] a) H. C. Liu, J. W. Zhong, C. K. Lee, S. W. Lee, L. W. Lin, *Appl. Phys. Rev.* **2018**, *5*, 041306; b) S. Banerjee, S. Bairagi, S. W. Ali, *Ceram. Int.* **2021**, *47*, 16402; c) W. C. Tian, Z. Y. Ling, W. B. Yu, J. Shi, *Appl. Sci.* **2018**, *8*, 645.
- [5] a) S. Priya, *IEEE Trans. Ultrason. Ferroelec. Freq. Control* **2010**, *57*, 2610; b) C. H. Choi, I. T. Seo, D. Song, M. S. Jang, B. Y. Kima, S. Nahm, T. H. Sung, H. C. Song, *J. Eur. Ceram. Soc.* **2013**, *33*, 1343.
- [6] T. Li, *Degree Thesis, Nanyang Technological University*, **2004**.
- [7] S. Gao, H. R. Ao, H. Y. Jiang, in *7th Annual Int. Conf. on Materials Science and Engineering, IOP Conf. Series: Materials Science and Engineering*, IOP Publishing Ltd, Hubei, China, publisher **2019**, 562, p. 012098.
- [8] S. W. Kim, T. G. Lee, D. H. Kim, K. T. Lee, I. Jung, C. Y. Kang, S. H. Han, H. W. Kang, S. Nahm, *Nano Energy* **2019**, *57*, 581.
- [9] S. Neiss, F. Goldschmidtboeing, M. Kroener, P. Woias, *J. Phys. Conf. Ser.* **2013**, *476*, 012035.
- [10] Y. Dong, T. Q. Yang, Z. Xiao, Y. Z. Liu, X. C. Wang, *J. Mater. Sci. Mater. Electron.* **2015**, *26*, 7921.
- [11] N. Putthongchai, T. Kulworawanichpong, P. Laoratanakul, S. Srilomsak, *Integr. Ferroelectr.* **2010**, *114*, 81.
- [12] H. Chen, C. Jia, C. Zhong, Z. H. Wang, C. S. Liu, in *IEEE Int. Symp. on Circuits and Systems (IEEE Cat. No.07CH37868)*, IEEE, Piscataway, NJ **2007**, p. 557.
- [13] T. B. Xu, E. J. Soichi, J. H. Kang, L. Zuo, W. L. Zhou, X. D. Tang, X. N. Jiang, *Smart mater. Struct.* **2013**, *22*, 065015.
- [14] K. S. Ramadan, D. Sameoto, S. Evoy, *Smart Mater. Struct.* **2014**, *23*, 033001.
- [15] A. Toprak, O. Tigli, *J. Microelectromech. Syst.* **2015**, *24*, 1989.
- [16] H. A. Sodano, J. Granstrom, J. Feenstra, K. Farinholt, in *Proc. SPIE 6525, Active and Passive Smart Structures and Integrated Systems*, SPIE-The International Society for Optical Engineering, San Diego, CA, USA **2007**, p. 652502.
- [17] a) H. G. Wei, H. Wang, Y. J. Xia, D. P. Cui, Y. P. Shi, M. Y. Dong, C. T. Liu, T. Ding, J. X. Zhang, Y. Ma, N. Wang, Z. C. Wang, Y. Sun, R. B. Wei, Z. H. Guo, *J. Mater. Chem. C* **2018**, *6*, 12446; b) S. Priya, S. Nahm, in *Lead-Free Piezoelectrics*, Springer, New York **2012**, Ch. 9.
- [18] H. Maiwa, W. Sakamoto, *Ferroelectrics* **2013**, *446*, 67.
- [19] W. S. Kang, J. H. Koh, *J. Eur. Ceram. Soc.* **2015**, *35*, 2057.
- [20] I. T. Seo, C. H. Choi, D. Song, M. S. Jang, B. Y. Kim, S. Nahm, Y. S. Kim, T. H. Sung, H. C. Song, *J. Am. Ceram. Soc.* **2013**, *96*, 1024.
- [21] a) A. T. Le, M. Ahmadipour, S. Y. Pung, *J. Alloys Compd.* **2020**, *844*, 156172; b) S. D. Mahapatra, P. C. Mohapatra, A. I. Aria, G. Christie, Y. K. Mishra, S. Hofmann, V. K. Thakur, *Adv. Sci.* **2021**, *8*, 2100864.
- [22] J. Briscoe, S. Dunn, *Nano Energy* **2015**, *14*, 15.
- [23] a) B. Kumara, S. W. Kima, *Nano Energy* **2012**, *1*, 342; b) F. R. Fan, W. Tang, Z. L. Wang, *Adv. Mater.* **2016**, *28*, 4283.
- [24] W. L. Deng, L. Jin, Y. Q. Chen, W. J. Chu, B. B. Zhang, H. Sun, D. Xiong, Z. K. Lv, M. H. Zhua, W. Q. Yang, *Nanoscale* **2018**, *10*, 843.
- [25] Y. B. Chu, L. X. Wan, G. W. Ding, P. Wu, D. L. Qiu, J. Pan, H. M. He, in *14th International Conference on Electronic Packaging Technology*, IEEE, Piscataway, NJ, USA, Dalian, China **2013**, p. 1292.
- [26] Z. Zhang, Y. Chen, J. S. Guo, *Phys. E: Low-Dimens. Syst. Nanostruct.* **2019**, *105*, 212.
- [27] Microfine Materials Technologies Pte Ltd, PZN-PT Single Crystal, www.microfine-piezo.com, (accessed: August 2020).
- [28] Z. B. Yang, J. Zu, *Energy Convers. Manage.* **2016**, *122*, 321.
- [29] D. A. V. D. Ende, H. J. V. D. Wiel, W. A. Groen, S. V. D. Zwaag, *Smart Mater. Struct.* **2012**, *21*, 015011.
- [30] a) Q. P. Wang, W. Dai, S. Li, J. A. S. Oh, T. Wu, *Mater. Technol.* **2020**, *35*, 675. b) R. Singh, B. D. Pant, A. Jain, *Microsyst. Technol.* **2020**, *26*, 1499.
- [31] a) J. C. Park, J. Y. Park, Y. P. Lee, *J. Microelectromech. Syst.* **2010**, *19*, 1215; b) Y. Li, D. Z. Yin, X. Y. Chenning, *J. Appl. Phys.* **2020**, *127*, 064104.
- [32] a) J. H. Zhao, X. J. Zheng, L. Zhou, Y. Zhang, J. Sun, W. J. Dong, S. F. Deng, S. T. Peng, *Smart Mater. Struct.* **21** (2012) 105006 (8pp); b) X. Y. Gao, C. R. Qiu, G. Li, M. Ma, S. Yang, Z. Xu, F. Li, *Appl. Energy* **2020**, *271*, 115193.
- [33] A. Daniels, A. Giuliano, M. L. Zhu, A. Tiwari, in *IEEE Int. Conf. on Green Computing and Communications and IEEE Internet of Things and IEEE cyber Physical and Social Computing*, IEEE, Piscataway, NJ **2013**, p. 1665.
- [34] H. W. Kim, S. Priya, K. Uchino, R. E. Newnham, *J. Electroceram.* **2005**, *15*, 27.
- [35] D. B. Zhu, S. Beeby, J. Tudor, N. White, N. Harris, in *Proc. Eurosensors XXV*, **2011**, *25*, 199.
- [36] B. Kathpalia, D. Tan, I. Stern, F. Valdes, S. Kim, A. Erturk, in *Proc. Comput. Sci.* **2017**, *109C*, 1060.
- [37] S. Asano, S. Nishimura, Y. Ikeda, T. Morita, H. Hosaka, *Sens. Actuat. A: Phys.* **2020**, *309*, 112000.
- [38] H. D. Li, C. Tian, Z. D. Deng, *Appl. Phys. Rev.* **2014**, *1*, 041301.
- [39] Y. B. Jeon, R. Sood, J. H. Jeong, S. G. Kim, *Sens. Actuators A* **2005**, *122*, 16.
- [40] C. K. Lee, in *SPIE Newsroom* **2010**, <https://doi.org/10.1117/2.1201009.003180>.

- [41] J. Chandwani, R. Somkuwar, R. Deshmukh, *Microsyst. Technol.* **2019**, 25, 3867.
- [42] P. Asthana, G. Khanna, *Int. J. Model. Simul. Sci. Comput.* **2020**, 11, 2050008.
- [43] M. Umeda, K. Nakamura, S. Ueha, *Jpn. J. Appl. Phys.* **1996**, 35, 3267.
- [44] M. Anwar, L. Hakim, N. Nadzri, in *IEEE 4th Int. Conf. on Smart Instrumentation, Measurement and Application*, IEEE, Piscataway, NJ **2017**, p. 1.
- [45] K. Gibbs, *The Forces on the Body During Walking and Running*, [http://www.schoolphysics.co.uk/age16-19/Medical%20physics/text/Walking\\_/\\_index.html](http://www.schoolphysics.co.uk/age16-19/Medical%20physics/text/Walking_/_index.html), (accessed: August 2020).
- [46] J. F. Nataki, G. E. Bertocci, E. C. Green, A. Nadeem, T. Rintoul, R. L. Kormos, B. P. Griffith, *Slide ASAIO Journal*, 41, pp. M588–M595.
- [47] L. Wang, D. J. Lu, Z. D. Jiang, C. Jia, Y. M. Wu, X. Y. Zhou, L. B. Zhao, Y. L. Zhao, *AIP Adv.* **2018**, 8, 115205.
- [48] G. W. Taylor, J. R. Burns, S. M. Kammann, W. B. Powers, T. R. Welsh, *IEEE J. Ocean. Eng.* **2001**, 26, 539.
- [49] S. F. Nabavi, A. Farshidianfar, A. Afsharfar, *Appl. Ocean Res.* **2018**, 76, 174.
- [50] J. W. Kan, C. T. Fan, S. Y. Wang, Z. H. Zhang, J. M. Wen, L. S. Huang, *Renew. Energy* **2016**, 97, 210.
- [51] M. Gratuze, S. Nabavi, A. H. Alameh, F. Nabki, *IEEE Sens.* **2019**, 1.
- [52] X. Luo, Y. B. Gianchandani, in *Sensors*, IEEE, Piscataway, NJ **2012**, p. 1.
- [53] T. Tanaka, *Ferroelectrics* **1982**, 40, 167.
- [54] a) S. I. Shkurov, E. F. Talantsev, J. Baird, in *Piezoelectric Ceramics*, (Eds: E. Suaste-Gomez), IntechOpen, London, UK **2010**, Ch. 14; b) M. S. Seo, J. Ryu, in *AIP Conf. Proc.*, Vol. 706 (Eds: M.D. Furnish, Y.M. Gupta, J.W. Forbes), **2004**, p. 1313.
- [55] a) R. A. Islam, S. Priyaw, *J. Am. Ceram. Soc.* **2006**, 89, 3147; b) R. A. Islam, S. S. Priyaa, *Appl. Phys. Lett.* **2006**, 88, 032903.
- [56] a) G. Q. Wang, X. L. Li, X. B. Wang, *J. Phys. Conf. Ser.* **2019**, 1303, 012097; b) S. Islam, A. Kim, in *IEEE Int. Microwave Biomedical Conference (IMBioC)*, IEEE, Piscataway, NJ **2018**, p. 70; c) N. S. Thakare, S. S. Thakare, R. S. Shahakar, in *3rd IEEE Int. Conf. on Recent Trends in Electronics, Information & Communication Technology (RTEICT)*, IEEE, Piscataway, NJ **2018**, p. 784.
- [57] a) Q. P. Wang, S. Li, J. A. S. Oh, T. Wu, *Mater. Technol.* **2020**, 35, 650; b) D. Floyd, M. Shafik, *Adv. in Manufact. Technol.* **2021**, XXXIV, 237; c) M. H. Yao, J. Li, Y. Niu, *Sens. Actuators A: Phys.* **2021**, 331, 112986.
- [58] K. Q. Fan, C. H. Xu, W. D. Wang, *Trans. Tianjin Univ.* **2014**, 20, 407.
- [59] a) N. Elvin, A. Elvin, D. H. Choi, *J. Strain Analysis* **2003**, 38, 115; b) S. Balguvhar, S. Bhalla, in *2nd Int. Conf. on Green Energy and Applications (ICGEA)*, IEEE, Piscataway, NJ, USA, Singapore **2018**, p. 134; c) L. Wang, L. B. Zhao, G. X. Luo, Y. H. Zhao, P. Yang, Z. D. Jiang, R. Maeda, *Sens. Actuators A* **2020**, 310, 112039; d) S. Townsend, S. Grigg, R. Picelli, C. Reatherston, H. A. Kim, *J. Intell. Mater. Syst. Struct.* **2019**, 30, 2894; e) F. Okosun, V. Pakrashi, *IEEE Int. Instrumentation and Measurement Technology Conf.*, IEEE, Piscataway, NJ **2020**, p. 1; f) H. Elahi, *Micorsyst. Technol.* **2021**, 27, 2605; g) S. X. Shi, Q. Q. Yue, Z. W. Zhang, J. Yuan, J. L. Zhou, X. K. Zhang, S. Lu, X. Luo, C. Y. Shi, H. Yu, *Micromachines* **2018**, 9, 629.
- [60] H. A. Sodano, G. Park, D. J. Leo, D. J. Inman, in *Proc. SPIE 5050, Smart Structures and Materials 2003: Smart Sensor Technology and Measurement Systems*, SPIE, San Diego, California, United States **2003**, <https://doi.org/10.1117/12.484247>.
- [61] A. M. Khalatkar, V. K. Gupta, *J. Renew. Sustain. Energy* **2017**, 9, 024701.
- [62] X. R. Zhou, K. Parida, O. Halevi, Y. Z. Liu, J. Q. Xiong, S. Magdassi, P. S. Lee, *Nano Energy* **2020**, 72, 104676.
- [63] a) M. Leinonen, J. Juuti, H. Jantunen, J. Palosaari, *Energy Technol.* **2016**, 4, 620; b) R. Meier, N. Kelly, O. Almog, P. Chiang, in *36th Annual Int. Conf. of the IEEE Engineering in Medicine and Biology Society*, IEEE, Piscataway, NJ **2014**, p. 622; c) Snehalika, M. U. Bhasker, in *IEEE 1st Int. Conf. on Power Electronics, Intelligent Control and Energy Systems (ICPEICES)*, IEEE, Piscataway, NJ **2016**, p. 1.
- [64] J. Rastegar, R. Murray, C. Pereira, H. L. Nguyen, in *Proc. SPIE 6527, Industrial and Commercial Applications of Smart Structures Technologies*, SPIE-The International Society for Optical Engineering, San Diego, CA, USA **2007**, p. 65270Y.
- [65] H. Zhang, K. X. Huang, Z. C. Zhang, T. Xiang, L. W. Quan, *J. Appl. Mech.* **2019**, 86, 091012.



**Li Tao** is a principal research fellow in School of Materials Science and Engineering, Nanyang Technological University. He works on piezoelectric materials, devices, and applications. His research interests include smart materials, smart structures, sensors, actuators, transducers, energy harvesters, micropump, micromotor, and so on.



**Pooi See Lee** is the President's Chair Professor in Materials Science and Engineering, Nanyang Technological University, Singapore. Her research focuses on nanomaterials for energy and electronics applications, flexible, and stretchable devices, electrochemical inspired devices, sensors and actuators, human-machine interface. She received her Ph.D. in 2002, Materials Science in National University of Singapore.